Laser-based fabrication of polymer micropump

Joohan Kim
Xianfan Xu
Purdue University
School of Mechanical Engineering
West Lafayette, Indiana 47907
E-mail: xxu@ecn.purdue.edu

Abstract. Diffuser micropumps are commonly fabricated using the standard lithography techniques with silicon as the base material. The important components of this type of micropumps are flow-directing diffusers and a moving diaphragm. Different diffuser designs show various flow rates and pump efficiency. In this work a polymer is used as the base material instead of silicon. It is demonstrated that polymer-based micropumps can be conveniently fabricated using the laser machining technique. Moreover, because of the flexibility of polymer materials, there is great potential to improve the performance of the polymer micropumps. The fluid flow inside the diffuser polymer micropump is also calculated using computational fluid dynamics methods and the simulated results are compared with the experimental data. [DOI: 10.1117/1.1631923]

Subject terms: micropump; laser machining; diffuser; polymer; microelectromechanical systems.

Paper 03042 received Apr. 22, 2003; revised manuscript received Aug. 13, 2003; accepted for publication Aug. 19, 2003. This paper is a revision of a paper presented at the SPIE conference on Microfluidics, BioMEMS, and Medical Microsystems, January 2003, San Jose, California. The paper presented there appears (unrefereed) in SPIE Proceedings Vol. 4982.

1 Introduction

The development of microelectromechanical systems (MEMS) has been driven by the need for miniaturization and lowering the overall manufacturing cost. Lasers have been used widely as a versatile manufacturing tool for decades and recently, research has been carried out in laser-based MEMS fabrication.[1,2] The laser fabrication technique is fast, clean, safe, and convenient compared with the photolithography process. Many traditional MEMS technologies are based on batch processes stemming from the microelectronic industry. However, one of its disadvantages is that the extensive fabrication process has to be repeated for any change of design parameters.[3] On the other hand, it is relatively easy to vary laser processing conditions for a different requirement, thus the laser technique is very suited for rapid prototyping.[4]

The microfluidic system is one of the applications of MEMS, and the micropump is a crucial device in a microfluidic system. Various types of micropumps have been developed. Earlier designs of micropumps were based on passive check valves.[5,6] When a diaphragm is actuated to supply fluid to a chamber, the inlet valve is open and the outlet valve is closed and the valve function is reversed when the diaphragm pumps the fluid to the outlet. This kind of pump has a high rectification efficiency, as defined for diffusion pumps (see later), which has a theoretical value of 1.0. However, fabrication of mechanical moving parts is complicated, and the probability of mechanical failure is high. As an alternative, valveless micropumps were proposed such as the electro-osmotic pump and the electrohydrodynamic pump for which electrokinetic phenomena are used to drive the fluid.[7–9] Normally, specific types of fluid are required for these pumps and the pumping efficiency depends on the ionic or charge level of the fluid, which limits the use of these pumps as a general purpose microfluidic device.[10]

The diffuser micropump is another type of valveless pump first demonstrated by Stemme and Stemme.[11] It consists of a chamber with a diaphragm, an inlet diffuser, and an outlet diffuser, as shown in Fig. 1. This valveless micropump has many advantages for microfluidic delivery compared with other micropumps. Most of all, its structure is quite simple. Only two diffusers and one chamber with a moving diaphragm are required to pump the fluid. The reliability of the system is also improved. Any type of fluids, liquid or gas, can be used as the working fluid.[12]

The efficiency of the diffuser micropump depends on many factors such as the diffuser angle, the diffuser length, the level of roundness of the edge of the diffuser, the properties of the fluid, and the Reynolds number (Re) in the diffusers.[13] If the Reynolds number in the diffusers is too low (less than 100), the efficiency deceases. The design must be optimized within the constraint of the supplying volume by the diaphragm. Most diffuser micropumps are fabricated using silicon as the base material using well-established technologies derived from the semiconductor industry. Recently, polymer has been proposed as an alter-

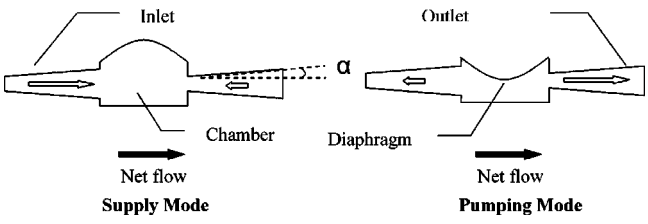

Fig. 1 Schematic diagram of a diffuser micropump with narrow angle diffusers; α is the diffuser angle.

 1537-1646/2004/$15.00

native material to replace silicon in the field of microfluidic devices including diffuser micropumps.[14,15] The key advantages of using polymer are as follows. First, it is cost-effective. Second, it has desirable material properties. Polymer is much less rigid than silicon; therefore, the diaphragm in the polymer micropump can be deflected easily which leads to improved pumping rate. Moreover, using transparent polymer materials for the pump improves optical visibility. Finally, it is easily machined using laser technology. Polymer pumps can also be reproduced with soft lithography or stamping methods.[16] In this work, laser machining of polymer is used to fabricate polymer-based diffuser micropumps. Flow rates are measured and compared with the pumps fabricated using other techniques.

2 Fabrication

As stated earlier, diffusers are key elements in the micropump studied in this work. A diffuser is a device that converts potential energy of a fluid into kinetic energy.[17] The performance of a diffuser micropump is normally characterized using a flow rectification efficiency ε, which can be calculated from the value of diffuser efficiency η, which is the ratio between the pressure loss coefficient at the diverging flow direction ξ_- and the pressure loss coefficient at the converging flow direction ξ_+:

$$\varepsilon = \frac{\sqrt{\eta}-1}{\sqrt{\eta}+1} = \frac{(\xi_-/\xi_+)^{1/2}-1}{(\xi_-/\xi_+)^{1/2}+1}, \tag{1}$$

where ε is a function of diffuser geometry, flow direction, and flow velocity because of the dependence of η on these parameters.[18] Two kinds of diffusers can be designed based on the peak values of ε: a diffuser with a wide angle (60 to 80 deg) and a narrow angle (4 to 10 deg). Diffuser micropumps with wide angles were fabricated on silicon wafers.[18–20] However, the rectification efficiency is not as high as that of a narrow-angle diffuser micropump due to the boundary layer separation along the diverging direction,[16] which does not occur in narrow-angle diffusers. For this reason, currently most diffuser micropumps use narrow-angle diffusers, which are shown to have a better pump efficiency.[21,22] In this work, micropumps are designed using narrow-angle diffusers.

In addition to optimizing the geometry of the diffusers, another way to improve the efficiency of the diffuser micropump is to increase the variation of the chamber volume. Using silicon as the base material, however, there is a limit of the variation of the chamber volume due to the rigidity of silicon. On the other hand, increasing the chamber volume variation can be easily achieved by using polymer as the diaphragm material. The deflection of the polymer diaphragm, which is proportional to the pumping rate in a certain pumping frequency range, could be much higher than silicon diaphragm.

In this work, the diffusers and the chamber are fabricated in 120-μm-thick Kapton films using laser ablation. Two laser machining techniques are employed: mask patterning and direct laser writing.[23] Mask patterning is very similar to photolithography except that it involves a single-step ''dry etching.'' A laser beam passes through a mask with a prefabricated pattern and irradiates the polymer surface using an imaging lens set. This technique can be applied if the patterned mask is available and its size is smaller than the laser beam. The direct writing method is also based on the imaging technique. The difference is that a primitive laser beam with a circular shape is imaged and scanned on the polymer surface. The polymer film moves according to pre-programmed paths using computer-controlled high-precision stages. A KrF excimer laser ($\lambda = 248$ nm) is used as a laser source to machine polymers. An optical imaging system, LightBench (Resonetics, Inc., Nashua, New Hampshire) with a three-element processing lens ($f = 88.4$ mm) forms 5 to 10 times demagnified images on the polymer surface. Laser fluences of 1.0 to 3.0 J/cm^2 and repetition rates of 1 to 8 Hz are used. Two masks, including pin holes of 300 and 600μm diameters are employed. The positioning stages have a 0.1-μm resolution and their moving speed varies between 1 and 10 μm/s. A CCD camera is installed on the LightBench to monitor the machining process.

Schematic diagrams of the diffuser micropump fabricated in this work is shown in Figs. 2 and 3. It consists of two Kapton layers, a glass substrate, an acrylic housing for inlet and outlet tubing, and an electromagnetic actuator. After the diffusers and the chamber are machined on one Kapton film, a glass substrate and another Kapton film are bonded to each side. The Kapton films have an adhesive layer on one side, which is used for assembly. An acrylic housing for installing an electromagnetic actuator and tubing is bonded to the second Kapton film layer with epoxy.

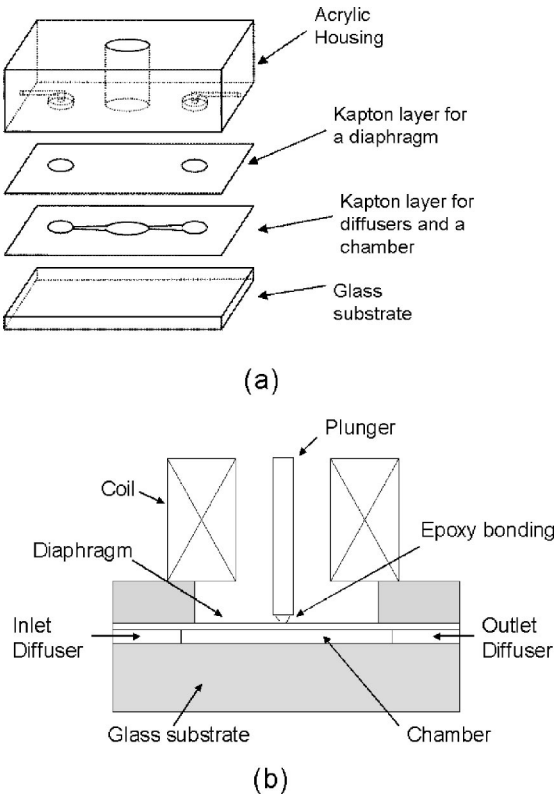

Fig. 2 (a) Perspective view of the diffuser polymer micropump and (b) side view of the pump assembly (not to scale).

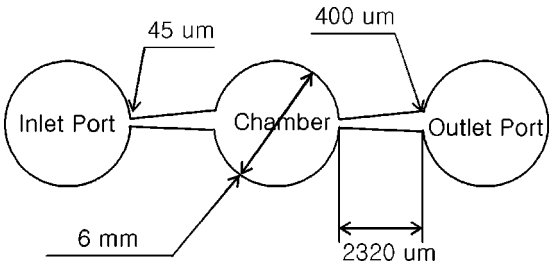

Fig. 3 Schematic of diffusers and the chamber (not to scale).

The width at the neck of the diffuser and the diffuser length are 45 and 2320 μm, respectively. The depth of the pump components is 120 μm. The angle of the diffusers is 9.8 deg, at which the diffusers show the highest rectification efficiency. The diameter of the chamber is 6 mm. Figure 4 shows the laser machined diffuser. An assembled diffuser polymer micropump with tubing is shown in Fig. 5.

3 Micropump Evaluation

The micropump is actuated using an external electromagnetic actuator (SD0420N, Bicron Electronics Co.), which consists of a magnet surrounded by a solenoid coil. The force from the magnet driven by the solenoid coil is used to drive the diaphragm of the membrane. A square wave (2 to 6 V) from a function generator is applied to the actuator. Deionized (DI) water is used as the fluid (viscosity $=1.002$ cP, density$=0.998$ kg/m^3 at 20 °C). The pump is first filled with DI water using a syringe. The deflection amplitude of the diaphragm as a function of actuation frequency is measured with the use of a HeNe laser and a position-sensitive detector (PSD). For this measurement, a tiny silicon piece is attached to the surface of the polymer diaphragm, as shown in Fig. 6. The motion of the diaphragm causes the position change of the HeNe laser beam reflected from the silicon, which is detected by the PSD, and the change is proportional to the deflection of the diaphragm. The measured deflections of the diaphragm from the oscilloscope at the frequency of 1 and 12 Hz are shown in Fig. 7. It is observed that the deflection occurs when the sign of the voltage is changed. The measured time duration of deflection is only 6 ms and the temporal shape is similar

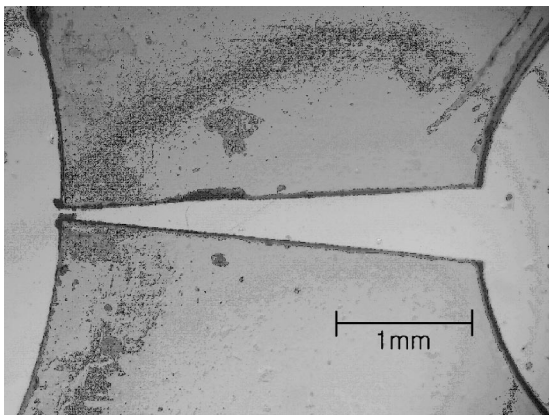

Fig. 4 Microscopic image of the diffuser.

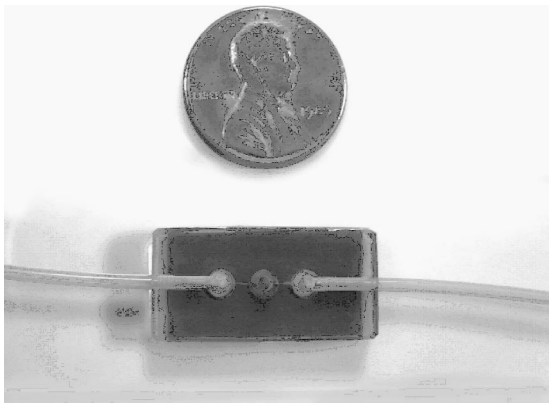

Fig. 5 Assembled diffuser polymer micropump.

to a parabola. This short time duration is a characteristic of the actuator used in this experiment, although the function generator outputs a longer pulse (half the period), as shown in Fig. 7. The time duration of deflection is almost constant when the frequency is below 160 Hz. The deflection magnitude in the rest of cycle is zero. The measured time-dependent diaphragm deflection is used in the numerical simulation and to explain the experimental data, as discussed in the following sections. Flow rate and pumping pressure as a function of frequencies are measured to evaluate the micropump performance. The flow rate is obtained by measuring the moving distance of small trapped bubbles in the transparent inlet and outlet tubing within a given time duration. The pumping pressure is obtained by measuring the difference of the water head between the inlet tubing and outlet tubing, similar to what was described in Ref. 24. Results of these measurements are presented later together with the results of numerical calculations.

4 Numerical Simulations

Numerical simulations of the fluid flow in the micropump are performed using a commercial computational fluid dynamics software FLUENT (FLUENT Inc., Lebanon, New Hampshire). The geometry of the pump is generated using a geometry modeling software GAMBIT provided with

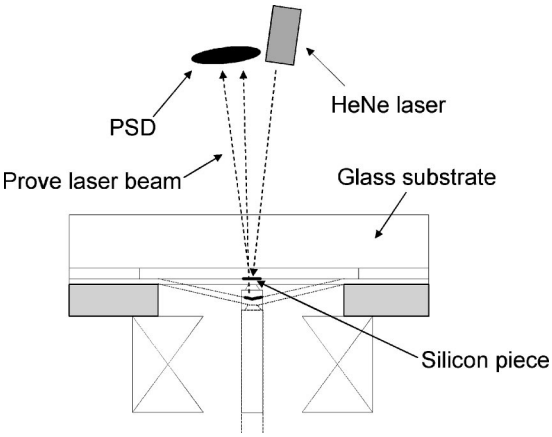

Fig. 6 Experimental setup for measuring the deflection of the diaphragm.

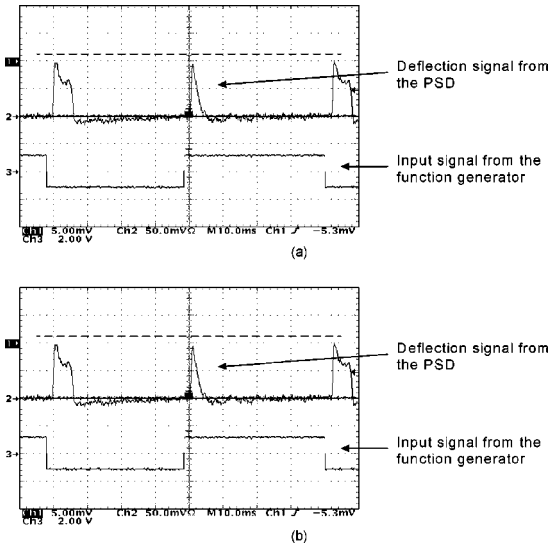

Fig. 7 Measured signals of the diaphragm deflection from the oscilloscope: (a) 1 and (b) 12 Hz.

FLUENT, and is shown in Fig. 8. The dimensions of the computational domain are exactly the same as those of the pump. Structured meshes and unstructured meshes are used for diffusers and the chamber, respectively. In the model, 44,375 hexahedral cells are generated. A moving boundary condition is applied to the upper wall of the chamber to simulate the motion of the diaphragm. Based on the measured deflection with respect to time, as shown in Fig. 9, the movement of the diaphragm is defined as follows:

$$z(x,y,t)=\begin{cases} A\cos\left[\dfrac{\pi}{2R}(x^2+y^2)^{1/2}\right]\sin(\omega t) & (0\leqslant t\leqslant 6\text{ ms}) \\ 0 & (t>6\text{ ms}), \end{cases} \tag{2}$$

where A is the amplitude at the center of the diaphragm, ω is the angular velocity, and R is the radius of the diaphragm. The time step used is 5×10^{-5} s. A constant pressure is applied at the inlet and outlet of the diffusers as the boundary conditions.

5 Results

Experimental results of the deflection amplitude of the diaphragm as a function of actuating frequency are shown in Fig. 10. The deflection amplitude is almost constant with

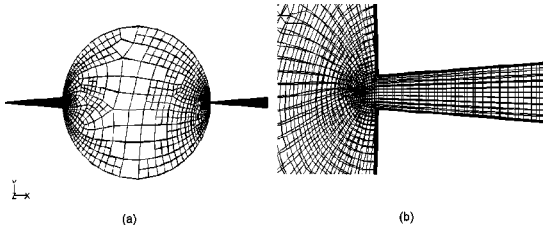

Fig. 8 Computational domain of the pump: (a) top view and (b) detailed meshes in the diffuser.

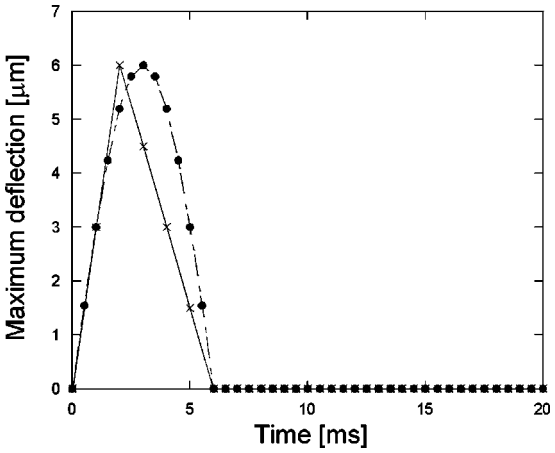

Fig. 9 Actual deflection of the diaphragm (×) and simulated maximum deflection (●) at the frequency of 1 Hz.

the frequency up to a frequency of about 130 to 140 Hz, and then decreases drastically. This is due to the characteristics of the electromagnetic actuator. This deflection is within its elastic region of polymer since it can deflect about 1 or 2 mm for a diaphragm with a diameter of 6 mm. At a frequency of about 140 Hz, pulses start to overlap with each other; and at frequencies higher than 180 Hz, a drastic decrease in the amplitude of the pulses is observed.

The volumetric flow rate and the pumping pressure with respect to the frequency are shown in Figs. 11 and 12. It is seen that the flow rate increases with the actuating frequency at low frequencies, but decreases drastically with the frequency after it reaches a maximum value due to the decrease in the deflection amplitude with the frequency, as shown in Fig. 11. The maximum volumetric flow rate and the pumping pressure are obtained at 180 Hz and are 50 mm^3/min and 380 Pa, respectively. At frequencies lower than 180 Hz, the volumetric flow rate increases almost linearly, which is due to the constant amplitude of the deflection of the diaphragm.

The pump rate obtained in this work is higher than some values reported in literature.[10,24,25] However, some

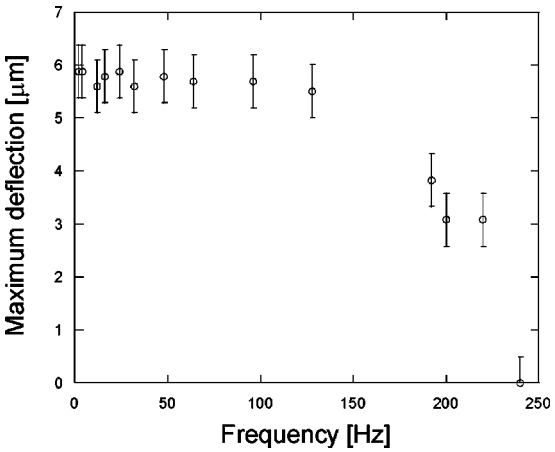

Fig. 10 Maximum deflection of the diaphragm as a function of frequency.

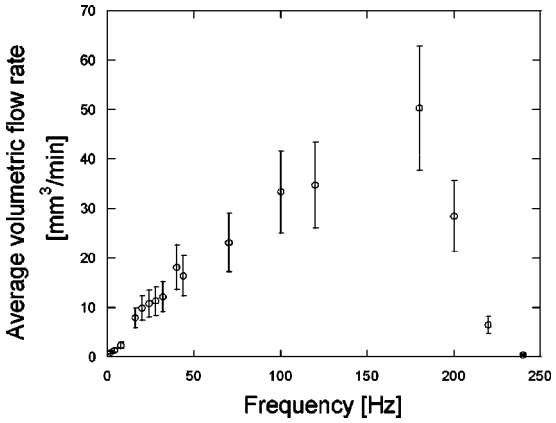

Fig. 11 Measured volumetric flow rate as a function of frequency.

researchers[12,14,16] reported flow rates in the range of milliliters per minute, which are obtained using a much higher pumping frequency approximately in the kilohertz range. On the other hand, it is believed that the pump rate of the polymer pump could be much improved with the use of a better actuating method. The actuating method used in this work only provides 6 μm of diaphragm deflection, while the maximum deflection allowed by this type of pump should be close to the height of the chamber, which is 120 μm. Large diaphragm deflections must be maintained at high frequencies as well, instead of what is shown in Fig. 10. Continuous actuation instead of short pulses can also improve the pumping efficiency at low frequencies. Currently, alternative actuating techniques are being investigated to further increase the pump rate.

Details of the fluid flow in the pump are obtained from the numerical simulation. The computed motion of the diaphragm using Eq. (2) is shown in Fig. 13. The net flow rates as a function of time in the first 10 ms are shown in Fig. 14. The pumping frequency is 1 Hz. Because the inlet flow rate is higher than the outlet flow rate in the supply mode and vice versa in the pump mode, the net flow rate is always positive. The simulated flow rate can be separated into two modes: the supply mode and the pump mode. At the beginning of the cycle, the supply mode, a large pumping force that is proportional to the acceleration of the diaphragm overcomes the inertia of the fluid to increase the flow rate to a certain level. Before reaching the maximum deflection of the diaphragm, the deacceleration of the diaphragm results in a decrease of the flow rate. At about 4 ms, the minimum flow rate is reached. In the pump mode, the flow rate increases again. After the diaphragm deflection stops at 6 ms, the flow rate decreases to zero within a few milliseconds. This indicates that the actuation method used in this work is not suited to obtain a high flow rate, particularly when the actuation rate is low. Ideally, the fluid flow should be continuous (although not constant) in the entire cycle. Flow rates using other types of actuation schemes are being calculated.

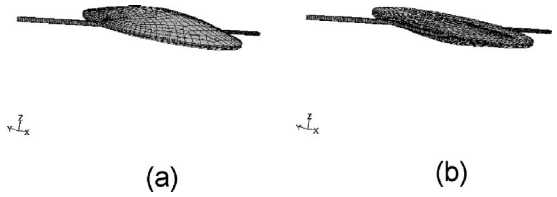

Fig. 13 A 3-D view of the working pump: (a) maximum deflection of the excited diaphragm for the supply mode and (b) maximum deflection of the diaphragm for the pump mode. The motion is exaggerated 10× for clarity.

Figure 15 shows velocity vectors in the chamber at 6 ms in the case of an actuating frequency of 1 Hz. As expected, the high velocity vectors are obtained in the narrow necks of the diffusers [Fig. 15(b)]. The calculated average velocity of the diffuser at the narrow neck is around 4.3 m/s, corresponding to a Reynolds number of 412. At this time, the average velocity over the cross section is the maximum. The velocity averaged over time is not calculated since during most of the time, there is no flow due to the short actuation duration (~6 ms) described previously. No vortexes can be observed inside of the chamber. It is also found that the neck pressures are 10 times higher than those in other zones.

The average flow rate can be calculated by integrating the transient flow rate in the cycle and is shown in the Fig.

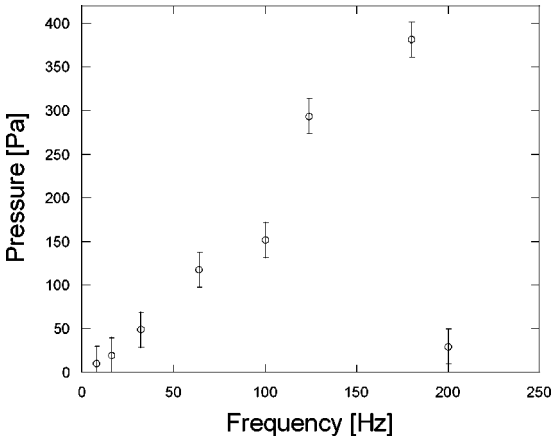

Fig. 12 Measured pumping pressure as a function of frequency.

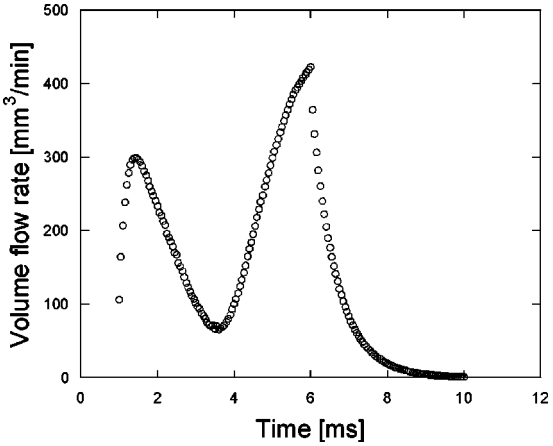

Fig. 14 Computed transient net volumetric flow rate at the frequency of 1 Hz.

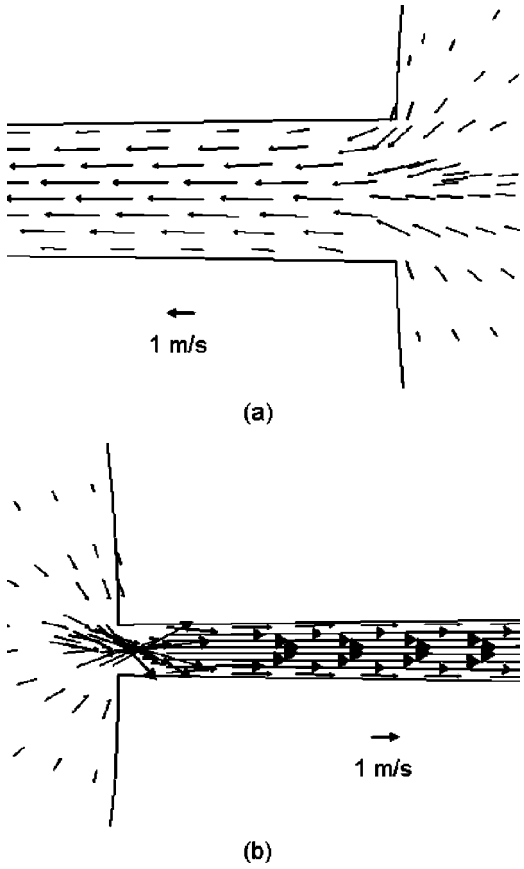

Fig. 15 Velocity vectors at the neck of the diffuser at 6 ms with an actuating frequency of 1 Hz: (a) right end of the diffuser and (b) left end of the diffuser.

16. The calculated average volume flow rate at 1 Hz is 2.67 mm^3/min, while the experimental result at this frequency is 0.97 mm^3/min. At other frequencies, the trend is similar except that the experimental results are higher than the numerical values by a factor of 3. A number of factors can cause this discrepancy. First, the numerical model does not consider the back pressure from the outlet and inlet reservoirs and water in the tubes. Imperfections of the laser-machined channels such as the surface roughness are also not modeled. In addition, trapping of bubbles from cavitations at high frequencies can be expected.[26] These factors all contribute negatively to the flow rate.

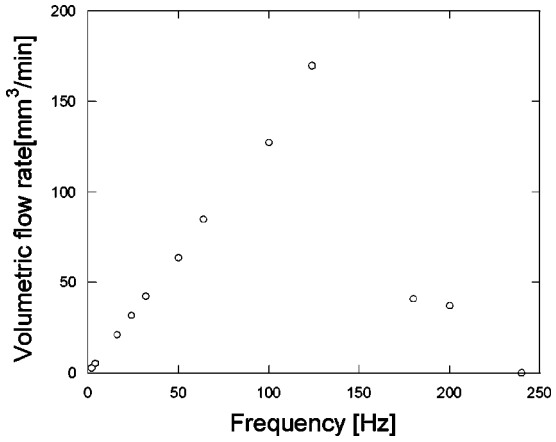

Fig. 16 Simulated volume flow rate with respect to frequency.

6 Conclusions

We employed the laser machining technique to fabricate valveless diffuser micropumps using polymer as the base material. The micropump showed a flow rate up to 50 mm^3/min at a frequency of 180 Hz. At higher frequencies, the flow rate decreased and no flow could be seen above 240 Hz because of the reduced deflection of the diaphragm at high frequencies. Simulation results using FLUENT were also presented. Compared with the experimental results, the numerical simulation showed the same trend of the pumping rate as a function of actuating frequency. The simulation results will be useful for designing different actuating methods to further improve the flow rate.

Acknowledgments

This work is supported by the Integrated Detection of Hazardous Materials (IDHM) Program, a Department of Defense project managed jointly by the Center for Sensing Science and Technology, Purdue University, and Naval Surface Warfare Center, Crane, Indiana. The authors also thank Sreemanth Uppuluri and Halil Berberoglu for their help in fabricating the diffuser polymer micropump and X. Richard Zhang for the deflection measurement.

References

1. S. Holmes and S. M. Saidam, ''Sacrificial layer process with laser-driven release for batch assembly operations,'' *J. Microelectromech. Syst.* **7**(4), 416–422 (1998).
2. J. Kim and X. Xu, ''Laser fabrication of micro-fluidic devices,'' in *Proc. ICALEO 2001*, pp. 1679–1688 (2001).
3. M. Lapczyna and M. Stuke, ''Rapid prototype fabrication of smooth microreactor channel systems in PMMA by VUV laser ablation at 157 nm for applications in genome analysis and biotechnology,'' *Mater. Res. Soc. Symp. Proc.* **526**, 143–148 (1998).
4. R. Vaidya, L. M. Tender, G. Bradley, M. J. O'Brein II, M. Cone, and G. P. Lopez, ''Computer-controlled laser ablation: a convenient and versatile tool for micropatterning biofunctional synthetic surfaces for applications in biosensing and tissue engineering,'' *Biotechnol. Prog.* **14**, 371–377 (1998).
5. P. Gravesen, J. Branebjerg, and O. S. Jensen, ''Microfluidics—a review,'' *J. Micromech. Microeng.* **3**, 168–182 (1993).
6. S. Shoji and M. Esashi, ''Microflow devices and systems,'' *J. Magn. Magn. Mater.* **4**, 157–171 (1994).
7. D. J. Harrison, A. Manz, and P. G. Glavina, ''Electroosmotic pumping within a chemical sensor system integrated on silicon,'' in *1991 IEEE Int. Conf. on Solid-State Sensors and Actuators, Digest of Technical Papers, Transducers'91*, pp. 792–795 (1991).
8. S. Zeng, C. Chen, J. C. Mikkelsen, Jr., and J. G. Santiago, ''Fabrication and characterization of electroosmotic micropumps,'' *Sens. Actuators B* **79**(2–3), 107–114 (2001).
9. S. F. Bart, L. S. Tavrow, M. Mehregany, and J. H. Lang, ''Microfabricated electrohydrodynamic pumps,'' *Sens. Actuators A* **21**(1–3), 193–197 (1990).
10. H. Andersson, W. van der Wijngaart, P. Nilsson, P. Enoksson, and G. Stemme, ''A valve-less diffuser micropump for microfluidic analytical systems,'' *Sens. Actuators B* **72**, 259–265 (2001).
11. E. Stemme and G. Stemme, ''A valveless diffuser/Nozzle-based fluid pump,'' *Sens. Actuators A* **39**, 159–167 (1993).
12. T. Gerlach and H. Wurmus, ''Working principle and performance of the dynamic micropump,'' in *Proc. IEEE Micro Electro Mechanical Systems (MEMS)*, pp. 221–226 (1995).
13. T. Gerlach, ''Microdiffusers as dynamic passive valves for micropump applications,'' *Sens. Actuators A* **69**, 181–191 (1998).
14. H. Becker and L. E. Locascio, ''Review polymer microfluidic devices,'' *Talanta* **56**, 267–287 (2002).
15. A. Olsson, O. Larsson, J. Holm, L. Lundbladh, O. Ohman, and G. Stemme, ''Valve-less diffuser micropumps fabricated using thermoplastic replication,'' *Sens. Actuators A* **64**, 63–68 (1998).

16. A. Olsson, P. Enoksson, G. Stemme, and E. Stemme, ''Micromachined flat-walled valveless diffuser pumps,'' *J. Microelectromech. Syst.* **6**(2), 161–166 (1997).
17. F. M. White, *Fluid Mechanics*, McGraw-Hill, New York (1979).
18. T. Gerlach, ''Aspects of stationary and dynamic micro diffuser flow,'' in *1997 IEEE Int. Conf. on Solid-State Sensors and Actuators, Digest of Technical Papers, Transducers'97*, Vol. 2, pp. 1035–1038 (1997).
19. T. Gerlach, M. Schuenemann, and H. Wurmus, ''A new micropump principle of the reciprocating type using pyramidic micro flowchannels as passives,'' *J. Micromech. Microeng.* **5**, 199–201 (1995).
20. T. Gerlach and H. Wurmus, ''Working principle and performance of the dynamic micropump,'' *Sens. Actuators A* **50**, 135–140 (1995).
21. A. Olsson, G. Stemme, and E. Stemme, ''A valve-less planar fluid pump with two pump chambers,'' *Sens. Actuators A* **46–47**, 549–556 (1995).
22. A. Olsson, G. Stemme, and E. Stemme, ''Diffuser-element design investigation for valve-less pumps,'' *Sens. Actuators A* **57**, 137–143 (1996).
23. J. Kim and X. Xu, ''Excimer laser fabrication of polymer microfluidic devices,'' *J. Laser Appl.* **15**(4), 255–260 (2003).
24. J.-H. Tsai and L. Lin, ''A thermal bubble actuated micro nozzle-diffuser pump,'' in *Proc. IEEE Micro Electro Mechanical Systems (MEMS)*, pp. 409–412 (2001).
25. M. Khoo and C. Liu, ''A novel micromachined magnetic membrane microfluid pump,'' in *Proc. 22nd Annu. Int. Conf. of the IEEE on Engineering in Medicine and Biology Society*, **3**, pp. 2394–2397 (2000).
26. R. W. Fox and A. T. McDonald, *Introduction to Fluid Mechanics*, John Wiley & Sons, New York (1998).

Joohan Kim received his BEng degree in 1996 and his MSc degree in 1997 in mechanical engineering from Ajou University and UMIST, respectively. He is currently working toward his PhD degree in the Center for Laser Micro-fabrication at Purdue University. His main interests are laser fabrication of polymer microfluidic devices and polymer replication techniques.

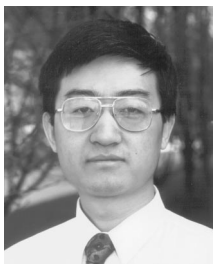

Xianfan Xu is an associate professor with the School of Mechanical Engineering and directs the Center for Laser Microfabrication of Purdue University. He received his MS and PhD degrees in mechanical engineering in 1991 and 1994, respectively, both from the University of California at Berkeley. His current research interests include laser micro- and nanofabrication and fundamental studies of laser material interactions.